TURBULENCE MODIFICATION IN A HOMOGENEOUS TURBULENT SHEAR FLOW LADEN WITH SMALL HEAVY PARTICLES

Mitsuru Tanaka
Dept. of Mech. and System Eng., Kyoto Inst. of Tech.
606-8585 kyoto, Japan
mtanaka@ipc.kit.ac.jp

Yasushi Maeda
Dept. of Mech. and System Eng., Kyoto Inst. of Tech.
606-8585 kyoto, Japan

Yoshimichi Hagiwara
Dept. of Mech. and System Eng., Kyoto Inst. of Tech.
606-8585 kyoto, Japan

ABSTRACT

Numerical simulations have been conducted for a homogeneous turbulent shear flow laden with small heavy particles in order to investigate the modification of turbulence structures in shear flows by particles. The effects on turbulence modification of particle drift due to gravity in the sheared direction are examined for particles with a response time comparable with the Kolmogorov time-scale of the turbulence. It is found that the growth rate of turbulence energy of the carrier fluid, which is reduced by the particles in zero gravity, is increased by the effect of weak gravity, but decreased by the effect of strong gravity. The interactions between concentrated regions of particles (particle clusters) and vortical structures are examined.

INTRODUCTION

Particle-laden turbulent shear flows are encountered in a variety of natural and engineering applications. Examples include combustion of sprays and ash from volcanic eruptions settling in the atmospheric turbulent boundary layer. Homogeneous turbulent shear flows laden with small heavy particles have been studied to deepen the understanding of the interaction between turbulent shear flows and particles within (Liljegren, 1993; Simonin et al., 1995; Mashayek, 1998; Ahmed and Elghobashi, 2000). Mashayek (1998) found that the presence of particles decreased the turbulence energy of the carrier fluid flow in the case without gravity. Ahmed and Elghobashi (2000) examined the modification of turbulence for particles in zero and finite gravities to find that the effect of gravity enhanced the growth of turbulence. They also investigated the modification of the vorticity dynamics by particles. However, the modification of vortical structures and their dynamics has not been examined in detail. In particular, no attentions have been focused on the shear layer (vortex layer) which is one of the major vortical structures in homogeneous turbulent shear flows (Kida and Tanaka, 1994).

In the present study, the accumulation of particles and turbulence modification in a homogeneous turbulent shear flow are examined by the use of a direct numerical simulation. We particularly focus on the interaction between vortical structures and clusters (concentrated regions) of particles, which may control the development of turbulence.

FORMULATION

Fluid and Particle Motions

We consider the motions of small heavy spherical particles in homogeneous turbulence subjected to the mean flow in the x_1 direction that is uniformly sheared in the x_2 direction, $\overline{\boldsymbol{u}} = (\gamma x_2, 0, 0)$, where γ is the shear

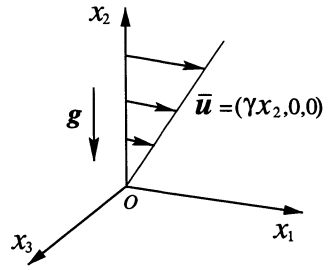

Figure 1: Configuration.

rate (see Fig. 1). The particle is assumed to be small enough, compared with the Kolmogorov length-scale l_K of the turbulence. Since we consider the particles of high density ratio, only Stokes drag and gravitational forces are assumed to act on the particles (Maxey and Riley 1983). In this study, we consider the gravity in the negative x_2 direction. The particulate phase is assumed to be dilute enough that the effects of particle-particle interactions are neglected, though the two-way interaction between two phases is taken into account.

Decomposing the total fluid velocity, u_i, as

$$u_i = \gamma x_2 \delta_{i1} + u_i', \tag{1}$$

the equation for fluctuating velocity, u_i', is written as

$$\frac{\partial u_i'}{\partial t} + \gamma x_2 \frac{\partial u_i'}{\partial x_1} + u_k' \frac{\partial u_i'}{\partial x_k} = -\gamma u_2' \delta_{i1} - \frac{1}{\rho_f}\frac{\partial p}{\partial x_i} + \nu \nabla^2 u_i' + f_i \tag{2}$$

with the solenoidal condition $\partial u_j'/\partial x_j = 0$, where ρ_f is the density, p is the pressure, and ν is the kinematic viscosity of the fluid. f_i represents a reaction force exerted by the particles on the fluid. The spatial average of f_i, which is generally non-zero, is assumed to be balanced by the mean pressure gradient.

The particle phase is tracked in the Lagrangian frame. The motion of the spherical particle with diameter, d_p, is described by

$$\frac{\mathrm{d}v_i}{\mathrm{d}t} = \frac{1}{\tau_p}\left(\widetilde{u}_i - v_i + V_{iS}\right), \quad \frac{\mathrm{d}x_i^{(p)}}{\mathrm{d}t} = v_i, \tag{3}$$

where $x_i^{(p)}$ and v_i denote the position and the velocity of the particle, respectively, and $\widetilde{u}_i = u_i(\boldsymbol{x}^{(p)})$ is the velocity of the surrounding fluid. τ_p is the particle response time, which is given by $\rho_p d_p^2/18\rho_f\nu$ for Stokes flow, where ρ_p is the density of the solid particles. $V_{iS} = \tau_p g_i = -V_S\delta_{i2}$ is the still-fluid terminal velocity of the particle due to the gravity, where $g_i = -g\delta_{i2}$ $(g > 0)$ denotes the gravity, and $V_S = \tau_p g$.

Decomposing the particle velocity as

$$v_i = \gamma x_2 \delta_{i1} + v_i', \tag{4}$$

we obtain the evolution equation for v_i' as

$$\frac{\mathrm{d}v_i'}{\mathrm{d}t} = \frac{\mathrm{d}}{\mathrm{d}t}(v_i' - \gamma x_2 \delta_{i1}) = -\gamma v_2' \delta_{i1} + \frac{1}{\tau_p}\left(\widetilde{u}_i' - v_i' + V_{iS}\right). \tag{5}$$

Equation (5) indicates that in a laminar simple shear flow the particle moves faster than the mean shear at the particle position by $v_1' = -\gamma\tau_p v_2' = \gamma\tau_p^2 g$ for $t \gg \tau_p$.

Turbulence Energy

The time development of turbulence kinetic energy of the carrier fluid, $E = (1/2)\langle u_k' u_k' \rangle$, is given by

$$\frac{\mathrm{d}E}{\mathrm{d}t} = -\gamma\langle u_1' u_2' \rangle - \epsilon + F, \tag{6}$$

where $\langle\ \rangle$ denotes the spatial average. The first and second terms represent the rate of turbulence energy production and the rate of turbulence energy dissipation, respectively. F denotes the energy transfer to the fluid phase due to the direct interaction with the particles through Stokes drag;

$$\begin{aligned} F &= (1/2)F_{kk}, \\ F_{ij} &= \left\langle f_i u_j' + f_j u_i' \right\rangle \\ &= \frac{\overline{C}}{\tau_p}\left\langle \widetilde{u}_i'(\widetilde{u}_j' - v_j') + \widetilde{u}_j'(\widetilde{u}_i' - v_i') \right\rangle_p, \end{aligned} \tag{7}$$

where $\overline{C}$ represents the particle volume fraction, and $\langle\ \rangle_p$ denotes the ensemble average over particles.

Numerical Method

Navier-Stokes equations were solved on 128^3 grid points in a rectangular box of sides $4\pi \times 2\pi \times 2\pi$, by using the Fourier spectral/ Runge-Kutta-Gill scheme, starting with random and isotropic initial conditions. The initial conditions were similar to those in Kida and Tanaka (1992,1994), but the small-scale resolution was improved.

We focused on the case of $\tau_p = \tau_K$, where τ_K is the Kolmogorov time-scale of the turbulence, and the effects of gravity were examined by changing the value of V_S as $V_S^+ \equiv \tau_K V_S/l_K = 0, 2, 4$. We introduced 2^{21} $(= 2097152)$ particles randomly throughout the computational domain at the non-dimensional time of $\gamma t = 4$

ρ_p/ρ_f	τ_p/τ_K	d_p/l_K
1000	1.0	0.134
$V_S\tau_K/l_K$	V_S/u'	$\overline{C}$
0,2,4	0,0.67,1.35	8.24×10^{-5}

Table 1: Particle parameters. Normalization is done using Kolmogorov scales and u' of the single-phase flow at $\gamma t = 8$.

where the turbulence had attained the quasi-equilibrium state (Kida and Tanaka, 1992). The particle volume fraction was as low as $\overline{C} = 8.24 \times 10^{-5}$. The parameters employed in this simulation are summarized in Table 1.

The initial particle velocity was set to be the same as the surrounding fluid velocity. Third order Lagrange interpolation was used both for the evaluation of fluid velocity at the particle position from its neighboring grid points and for the distribution to the grid points of the reaction force exerted by the particle on the fluid (Sundaram and Collins, 1996). $k_{\max}l_K$ was 1.80 at $\gamma t = 4$, where $k_{\max} = N/2$ ($N = 128$). The particle Reynolds numbers remained less than unity throughout the simulations.

RESULTS

Turbulence Energy

Figure 2 shows the time development of turbulence kinetic energy of the carrier fluid flow which is normalized by the value at the time of particle injection ($\gamma t = 4$). As reported before (Kida and Tanaka, 1992), the turbulence energy in the single-phase flow increases exponentially in time. It is seen that the growth of turbulence energy is suppressed by the injection of the particles in zero gravity as was shown in Mashayek (1998). The increase in the gravity leads to an increase in the turbulence energy for the case of $V_S^+ = 2$, which is in agreement with the result in Ahmed and Elghobashi (2000). However, a further increase of the gravity again brings about the attenuation of the growth rate of turbulence ($V_S^+ = 4$).

In order to examine the mechanisms of the turbulence modification, we consider the budget for the turbulence kinetic energy (Eq. (6)). Figure 3 shows the time development of the non-dimensional growth rate of energy, $(1/E)\mathrm{d}E/\mathrm{d}(\gamma t)$. In addition, the production (first), the dissipation (second), and the phase-interaction (third) terms in the right-hand-side of Eq. (6) are plotted in Fig. 3. These three terms are also non-dimensionalized by multiplying $1/\gamma E$. The attenuation of turbulence in zero gravity is triggered mainly by the decrease in the production of turbulence energy, though the phase-interaction term also play a role to decrease the energy particularly in a later period when the effective particle inertia, τ_p/τ_K, becomes larger. It is found that the presence of particles reduces the energy production, $-\gamma\langle u_1' u_2'\rangle$, directly through the phase-interaction term, $-\gamma F_{12}$ and indirectly through the suppression of the production term, $\gamma^2\langle u_2' u_2'\rangle$, in the evolution equation of $-\gamma\langle u_1' u_2'\rangle$ (not shown here).

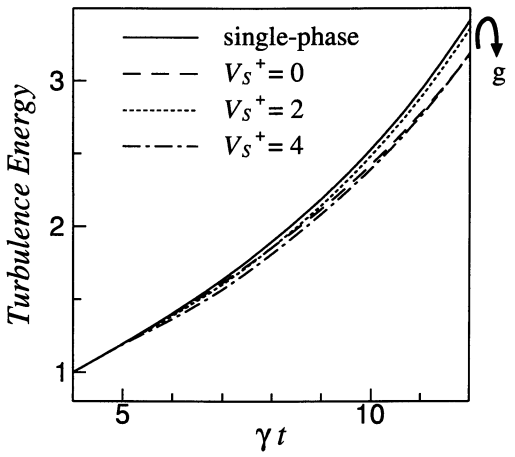

Figure 2: Time development of turbulence kinetic energy of the carrier fluid flow.

The energy production increases with gravity. The enhancement of turbulence at $V_S^+ = 2$ is caused by this increase of Reynolds shear stress. The phase-interaction term, on the other hand, takes large negative values for $V_S^+ \gg 1$, which suppresses the development of turbulence, particularly in an initial period.

The phase-interaction term acts on the fluid differently depending on the directions. Figure 4 shows the time development of the phase-interaction term, F_{ii}, which is source/sink term due to particles in the evolution equation of $\langle u_i' u_i'\rangle$. In the case of zero gravity, the streamwise component, F_{11}, takes larger values compared with the other two component, F_{22} and F_{33}, which is consistent with previous finding (Liljegren, 1993; Simonin et al., 1995) that the effect of mean shear enhances the streamwise particle velocity variance. With the increase of gravity, the vertical component increases, but the streamwise and spanwise components decrease significantly. It is found that this is due to the crossing trajectories effects (Scanady, 1963), which reduce the streamwise and spanwise components of particle velocity variance.

Vorticity Dynamics

The time development of turbulence enstrophy, $\langle\omega_k'\omega_k'\rangle$, is shown in Fig. 5, where $\omega_i' = \epsilon_{ijk}\partial u_k'/\partial x_j$ denotes the fluctuating vorticity.

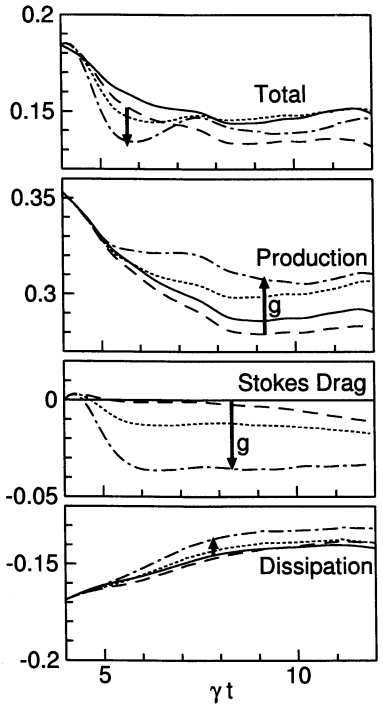

Figure 3: Time development of the growth rate of turbulence kinetic energy and contributions to the growth rate from the production, dissipation and phase-interaction terms. — single-phase, – – $V_S^+ = 0$, $\cdots$ $V_S^+ = 2$, – · – $V_S^+ = 4$.

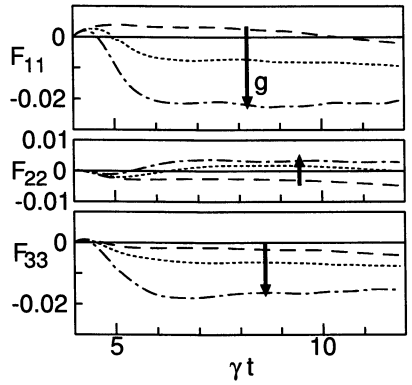

Figure 4: Time development of F_{ii} (Eq.(7)). — single-phase, – – $V_S^+ = 0$, $\cdots$ $V_S^+ = 2$, – · – $V_S^+ = 4$.

Figure 5 shows that the presence of particles in zero gravity enhances the enstrophy slightly in the initial instant, but suppresses it significantly in the later period ($\gamma t > 7$). The enstrophy is reduced further for $V_S^+ = 4$.

The particles modulate the vorticity field in an anisotropic manner. Figure 6 shows the time development of the anisotropy tensor of vorticity field, $w_{ij} = \left\langle \omega_i' \omega_j' \right\rangle / \left\langle \omega_k' \omega_k' \right\rangle - (1/3)\delta_{ij}$. The presence of particles in zero gravity reduces the relative magnitude of streamwise vorticity w_{11}, and increases that of spanwise vorticity w_{33}. In finite gravity, the injection of particles leads to the increase in w_{22} and w_{12}, and to the decrease in w_{33}.

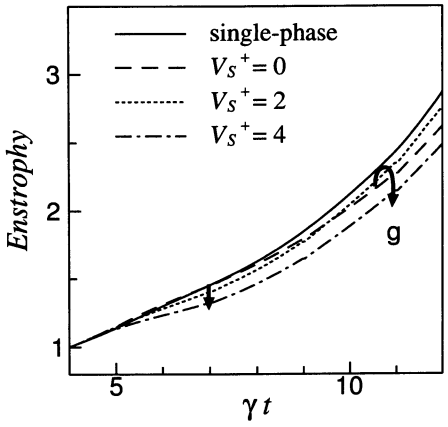

Figure 5: Time development of turbulence enstrophy.

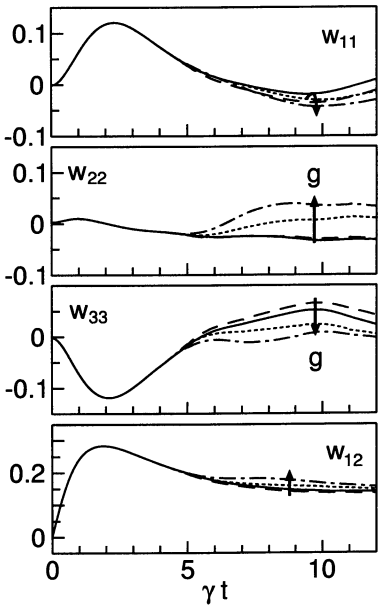

Figure 6: Time development of vorticity anisotropy tensor. — single-phase, – – $V_S^+ = 0$, $\cdots$ $V_S^+ = 2$, – · – $V_S^+ = 4$.

To examine the directional distribution of vorticity vectors more in detail, we introduce the orientation angles α and β of vorticity vector, which are defined as (Kawahara et al., 1997)

$$\begin{aligned} \omega_1 &= |\boldsymbol{\omega}| \cos\alpha \\ \omega_2 &= |\boldsymbol{\omega}| \sin\alpha \cos\beta \\ \omega_3 &= |\boldsymbol{\omega}| \sin\alpha \sin\beta. \end{aligned} \tag{8}$$

Figure 7 shows the probability density function (pdf) of orientation angles α and β of the vorticity weighted by $|\boldsymbol{\omega}^2|$, that is, the directional distribution of the enstrophy. Each pdf is normalized by the average value of the pdf in the case of the single-phase flow, and the average value (contour line of level 1) is represented by the bold line. The peak in the center ($\alpha = \pi/2, \beta = -\pi/2$) of each figure corresponds to the vortex layers with negative spanwise vorticity (Kida and Tanaka, 1994). The

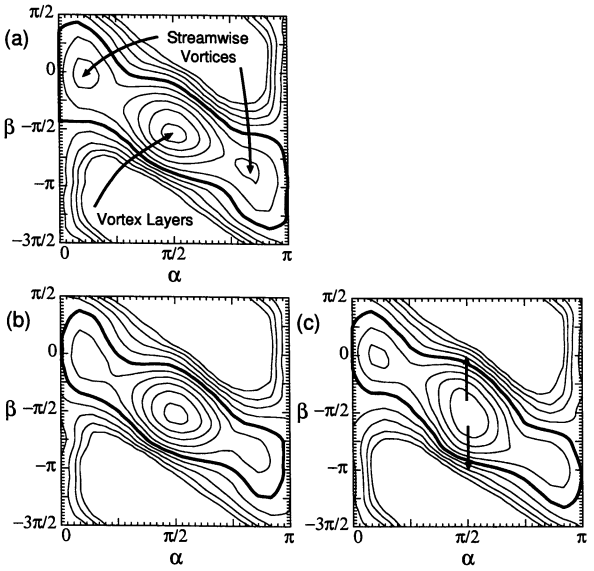

Figure 7: Directional distribution of enstrophy at $\gamma t = 12$ for (a) single-phase flow, (b) $V_S^+ = 0$ and (c) $V_S^+ = 2$. Contour levels are 2^p ($p = -4, -3.5, -3, ...$). The bold line represents the contour line of level 1.

other two peaks located at ($\alpha \approx \pi/8, \beta = 0$) and ($\alpha \approx 7\pi/8, \beta = -\pi$) correspond to streamwise vortices which are inclined toward the x_2 direction from the x_1 direction.

Comparing Figs. 7(a) and 7(b), we notice that the peak values of the pdf corresponding to streamwise vortices become smaller by the presence of particles in zero gravity. The peak corresponding to vortex layers, on the other hand, takes a slightly larger value than that in the single-phase flow. This indicates that the streamwise vortices are attenuated, while the vortex layers are intensified. This is consistent with the results of Druzhinin (1995a, 1995b). For $V_S^+ = 2$, the streamwise vortices are intensified compared with the case of $V_S^+ = 0$. Another distinguished feature in finite gravity is the modification of the enstrophy distribution around the peak corresponding to the vortex layers. The distribution is elongated in the $\pm x_2$ direction ($\alpha = \pi/2, \beta = 0, -\pi/2$) as is denoted by arrows, which corresponds to the deformation (bending) of vortex layers due to particle clusters (see Fig. 8 below).

Interaction between Vortical Structures and Particle Clusters

We have examined the interactions of particle clusters with vortical structures in order to identify the processes which control the aforementioned phenomena. Shaded regions in Fig. 8 indicate the cross sections of high concentrated regions of the particles for the case of $V_S^+ = 2$. The darker and lighter shades denote the regions of $C \geq 2\overline{C}$ and $C \geq \overline{C}$, respectively, where C denotes the local volume fraction of particles. Solid (broken) lines represent quasi-streamwise vortices which induce flows rotating clockwisely (counter-clockwisely). Here, we focus on three counter-rotating vortex pairs, A,B1,B2, marked by bold broken lines. Bold solid line represents a vortex layer of negative spanwise vorticity. The two vortex pairs, B1 and B2, induce a strong straining flow between them, which stretches the mean spanwise vorticity, as indicated by arrows, to generate the vortex layer. This is one of the typical vortical structures in homogeneous turbulent shear flows (Kida and Tanaka, 1994).

The settling particles are found to accumulate typically on two types of regions. We notice that the particles are concentrated to the downward fluid between the vortex pair A as in the case of isotropic turbulence (Wang and Maxey, 1993). Another type of particle cluster, which is rather horizontal, is found along the vortex layer. Note that this particle cluster is located beneath the vortex layer owing to the gravitational settling.

In Fig. 8(b), regions of high Reynolds shear stress, $-\gamma \langle u_1' u_2' \rangle \geq 0.05$, are represented by light shades for the single-phase flow on the same plane as Fig. 8(a). It is seen that the Reynolds shear stress takes large values in the area between the pair vortices A (Kida and Tanaka, 1992; Ahmed and Elghobashi, 2000). In the case of zero gravity, the Reynolds shear stress is attenuated (not shown) because the vortex pair A is weakened by the particle cluster. In the case of $V_S^+ = 2$, to the contrary, the Reynolds shear stress is enhanced in the region A (Fig. 8(c)). This is because the successive passing of particle clusters have intensified the downward flow between the pair vortices.

In Fig. 8(d), dark shades denote the regions of large negative values of the direct energy transfer by the particles (F in Eq.(6)). It is seen that the transfer takes large negative values in the area beneath the vortex layer. It is found that this negative transfer mainly comes from the streamwise component, F_{11} (not shown). In the vortex layer, the streamwise component of the fluid velocity decreases sharply in the gravitational (negative x_2) direction. Thus, because of their inertia, the settling particles slip (relative to the surrounding fluid) in the positive streamwise direction (see Eq.(5)). Since, in general, the streamwise component of fluctuating fluid velocity is negative beneath the vortex layer, the drag forces in

the positive streamwise direction act to reduce the amplitude of the streamwise fluid velocity.

Conclusion

We have carried out the DNS for a homogeneous turbulent shear flow laden with small heavy particles and obtained the following results:

(1) In the case of zero gravity and moderate particle inertia, the presence of particles decreases the turbulence kinetic energy of the fluid phase. At a finite value of gravity ($V_S^+ = 2$), the gravity enhances the Reynolds shear stress and the turbulence energy. At a larger value of gravity ($V_S^+ = 4$), the fluid turbulence is attenuated by the direct energy exchange with the particles.

(2) The particles tend to accumulate on the two types of regions. The interaction of the particle clusters with the vortical structures in these two regions seem to be important for the dynamics of the particle-laden turbulent shear flow.

REFERENCES

Ahmed, A.M. and Elghobashi, S., 2000, *Phys. Fluids*, Vol. 12, pp.2906-2930.

Csanady, G.T., 1963, *J. Atmos. Sci.*, Vol. 20, pp.201-208.

Druzhinin, O.A., 1995a, *J. Fluid Mech.*, Vol. 297, pp.49-76.

Druzhinin, O.A., 1995b, *Phys. Fluids*, Vol. 9, pp.2132-2142.

Kawahara, G., Kida, S., Tanaka M., and Yanase, S., 1997, "Wrap, tilt and stretch of vorticity lines around a strong thin straight vortex tube in a simple shear flow", *J. Fluid Mech.*, Vol. 353, pp.115-162.

Kida, S. and Tanaka, M., 1992. *J. Phys. Soc. Japan*, Vol. 61, pp.4400-4417.

Kida, S. and Tanaka, M., 1994, *J. Fluid Mech.*, Vol. 274, pp.43-68.

Liljegren, L.M., 1993, *Int. J. Multiphase Flow*, Vol. 19, pp.471-484.

Mashayek, F., 1998, *J. Fluid Mech.*, Vol.367, pp.163-203.

Maxey, M.R. and Riley, J.J., 1983, *Phys. Fluids*, Vol. 26, pp.883-889.

Sundaram, S. and Collins, L. R., 1996, *J. Comput. Phys.*, Vol. 124, pp.337-350.

Simonin, O., Deutsch, E. and Bovin, M., 1995, Turbulent Shear Flows 9, pp.85-115.

Wang, L.P. and Maxey, M.R., 1993, J. *Fluid Mech.* Vol.256 pp.27-68.

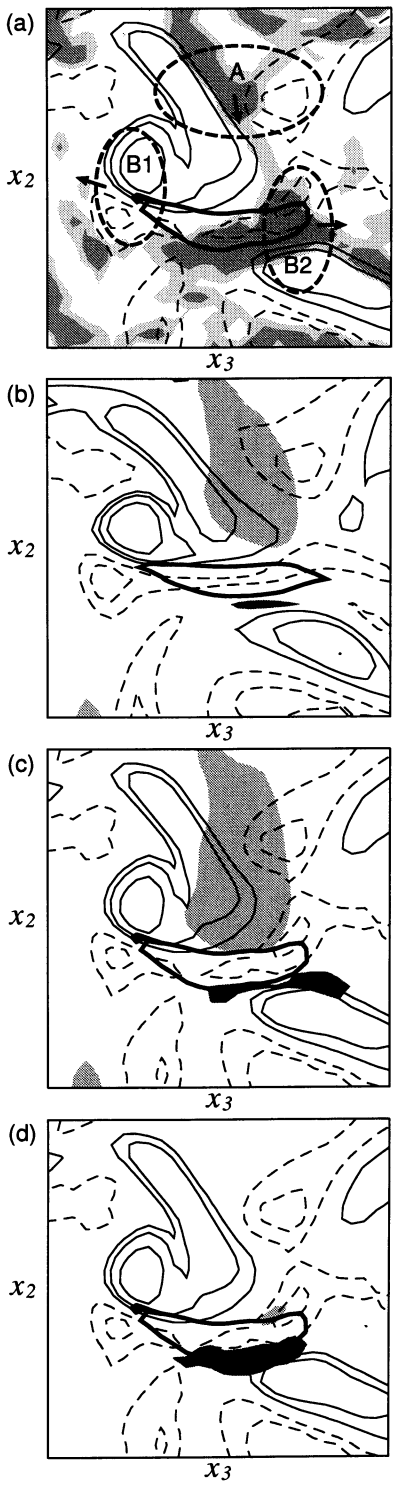

Figure 8: Typical example of the interactions between particle clusters and vortical structures at $\gamma t = 11$. (a) $V_S^+ = 2$. Darker and lighter shades denote the regions of $C \geq 2\overline{C}$ and $C \geq \overline{C}$, respectively. Contour lines of $\omega_1' = \pm\gamma, \pm 2\gamma, \pm 4\gamma$ are represented by thin solid and broken lines. Bold solid line represents the regions of $\omega_3' \leq -3\gamma$. Thick broken lines denote the counter-rotating vortex pairs. (b) The same as (a) but for the single-phase flow. Light and dark shades denote the regions of $-\gamma u_1 u_2 \geq 0.05$ and $-\gamma u_1 u_2 \leq -0.05$, respectively. (c) The same as (b) but for $V_S^+ = 2$. (d) The same as (c) except that light and dark shades denote the regions of $F \geq 0.05$ and $F \leq 0.05$, respectively.